Robotic Pick-And-Place of Multiple Embryos for Vitrification

Zhuoran Zhang, Jun Liu, Xian Wang, Qili Zhao, Chao Zhou, Min Tan, Huayan Pu, Shaorong Xie, and Yu Sun

***Abstract*—Embryo vitrification is an essential cryopreservation technique in IVF (*in vitro* fertilization) clinics. Vitrification involves pick-and-place of an embryo in multiple types of cryoprotectant solutions for processing before placing the embryo on a vitrification straw for cryopreservation in liquid nitrogen. Manual operation and existing robotic vitrification are only capable of aspirating one embryo at a time for processing; thus, other embryos are kept in the culture dish on a microscope stage for tens of minutes, which is detrimental to the development potential of the embryos. In order to minimize the total vitrification time, we have recently developed a robotic system for the pick-and-place of multiple embryos and process every three embryos as a group. Visual detection algorithms were developed for locating multiple embryos in three dimensions. Dynamics of embryo motion was modeled and a linear quadratic regulator (LQR) controller was developed to aspirate each embryo with a minimum volume of excess medium. The robotic system then placed the embryos onto vitrification straws by depositing a thin layer of medium that contains the embryos, and finally, aspirated away the medium surrounding the embryo for fast cooling. Experimental results demonstrate that robotic multiembryo processing has a throughput three times that of manual operation and achieved a high success rate of 95.2%, embryo survival rate of 90.0%, and development rate of 88.8%.**

***Index Terms*—Automation at Micro-Nano Scales, Biological Cell Manipulation.**

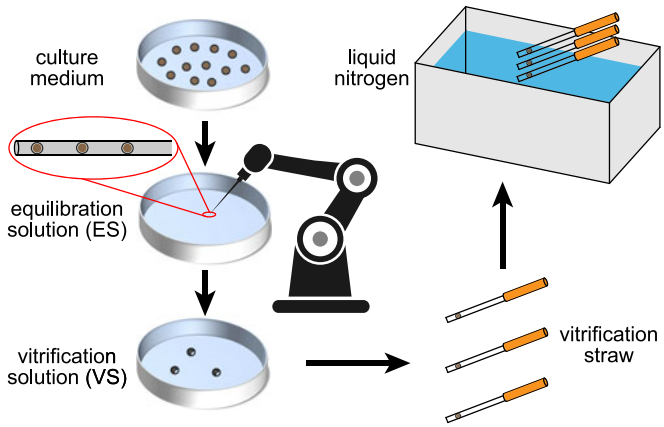

Fig. 1. Sequence of embryo vitrification (not drawn to scale). Manual operation is only capable of processing one embryo at a time. The robotic technology reported in this paper has a throughput three times that of manual operation, reducing the time embryos are kept outside the incubator environment and resulting in higher embryo survival rate. Red circle shows three embryos are aspirated by the robotic system into the micropipette with equal spacing.

I. Introduction

EMBRYO cryopreservation is widely used in IVF clinics [1]. Embryos are routinely frozen and cryopreserved globally to benefit patients. For instance, it allows child-bearing age cancer patients to reproduce at a later time as treatments (e.g., chemotherapy) can seriously compromise their reproductive ability. Due to professional/career choices, working women who decide to defer child-bearing to a later age can choose to have their embryos vitrified and stored.

Cryopreservation techniques are classified into two categories, including vitrification and slow freezing. Vitrification or fast freezing is a proven more effective method than slow freezing because it vitrifies the embryo with no ice crystal formation during freezing, hence, higher cell survival rates [2]. Vitrification involves pick-and-place of embryos in different types of cryoprotectant solutions. As shown in Fig. 1, an embryo is picked up from the culture medium, washed in the equilibration solution (ES), and then washed in the vitrification solution (VS), both with stringent timings. VS contains cryoprotectant agents such as dimethyl sulfoxide or ethylene glycol which creates an osmotic imbalance across the cell membrane and draws water molecules out of the embryo [3]. Dehydration changes the density of the embryo, causing embryos to float three-dimensionally in VS [4]. Dehydrated embryos are placed on vitrification straws (one embryo per straw) and plunged into liquid nitrogen for freezing and cryopreservation. The time from picking up embryos in the VS solution to depositing embryos on straws and aspirating away excess VS solution from the straw surface must

Manuscript received September 10, 2016; accepted December 10, 2016. Date of publication December 15, 2016; date of current version January 25, 2017. This paper was recommended for publication by Associate Editor N. Vahrenkamp and Editor T. Asfour upon evaluation of the reviewers' comments. This work was supported in part by the Natural Sciences and Engineering Research Council of Canada via an Idea to Innovation grant and the University of Toronto via a Connaught Innovation Award, in part by the National Natural Science of China under Grant 61528304, and in part by the Shanghai Municipal Science and Technology Commission Project (14JC1491500). Zhuoran Zhang and Jun Liu contributed equally to this work.

Z. Zhang, J. Liu, X. Wang, Q. Zhao, and Y. Sun are with the Department of Mechanical and Industrial Engineering, University of Toronto, Toronto, ON M5S 3G8, Canada (e-mail: sun@mie.utoronto.ca).

C. Zhou and M. Tan are with the Institute of Automation, Chinese Academy of Sciences, Beijing 100190, China (e-mail: zhouchao@compsys.ia.ac.cn; min.tan@ia.ac.cn).

H. Pu and S. Xie are with the Department of Mechatronic Engineering, Shanghai University, Shanghai 200072, China (e-mail: phygood_2001@shu.edu.cn; srxie@shu.edu.cn).

Color versions of one or more of the figures in this letter are available online at http://ieeexplore.ieee.org.

Digital Object Identifier 10.1109/LRA.2016.2640364

be minimized to avoid unnecessary overexposure of embryos to the toxic VS solution [5].

In manual vitrification, a highly skilled embryologist looks through the microscope eyepieces and manipulates embryos with intense focus. Manual operation by embryologists can only process a single embryo in each step with a limited throughput (∼15 minutes per embryo). In embryology, multiple embryos are cultured in the same culture dish, which is known to result in a higher development rate than culturing one embryo per dish [6], [7]. In manual vitrification, when one embryo is processed, the rest of the embryos have to wait for tens of minutes out of the incubator environment. Due to embryo's high sensitivity to the culture environment such as oxygen level [8], temperature [9] and osmolarity [10], this long waiting time can be detrimental to the development potential of the embryos. In addition, manual vitrification is a laborious and demanding task; and due to poor reproducibility and inconsistency across embryologists, success rates and cell survival rates also vary significantly [11].

Efforts have been made to automate the vitrification process. Microfluidic devices were developed for embryos washing [12], [13]; however, loss of embryos can occur during the retrieval of vitrified embryos from the microfluidic devices. We previously developed a robotic vitrification system [14] that was able to pick and place a single embryo at a time. In this work, we further developed our robotic vitrification system to achieve automated vitrification of multiple embryos. The new system achieved multi-embryo vitrification with the following new techniques: (1) algorithms for detecting and locating multiple embryos in 3D; (2) aspirating multiple embryos and accurate control of the multiple embryo positions; (3) utilizing both surface tension and friction force to deposit embryos on vitrification straws.

II. System Overview

A. System Setup

The system is built around a compact inverted microscope (Nikon Eclipse TS100) that is equipped with an X-Y motorized stage and motorized focusing (ProScan, Prior Scientific Inc.) [see Fig. 2(a)]. A custom designed carrier plate is placed on the X-Y stage to hold the culture dish (35-millimeter petri dish), multiwell dish (universal GPS dish, The LifeGlobal Group) containing the ES and VS solutions, and vitrification straws (Cryotop, Kitazato Corporation) [see Fig. 2(a) inset]. A micropipette (tip diameter: 125 μm) is mounted on a micromanipulator (MP285, Sutter Inc.) to manipulate embryos. The micropipette is connected to a pump (CellTram Vario, Eppendorf Canada Ltd.) which is controlled by a stepper motor (Phidgets Inc.). A camera (Basler scA 1300-32gm) is connected to the microscope to obtain visual feedback. Images are captured in brightfield at 30 frames per second with a 2X objective. Fig. 2(b) summarizes the system control architecture. Visual feedback of 3D embryo positions is used to form a visual servo control system. The motorized syringe pump, X-Y stage, focusing (z) motor, and micromanipulator are cooperatively controlled for the pick-and-place of embryos.

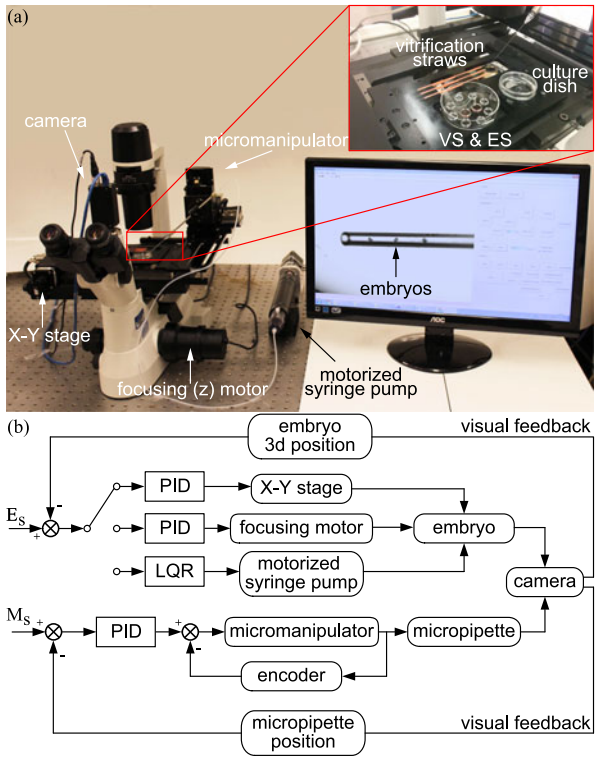

Fig. 2. (a) Robotic vitrification system setup. Inset shows the custom designed carrier plate which holds the culture dish, multiwell dish, and vitrification straws. (b) System control architecture. Embryo positions are detected from visual feedback. M_s is the target position for the micropipette for picking up embryos three dimensionally and placing embryos on vitrification straws. E_s is the target position of embryos, and different control tasks are switched according to controlled aspiration of embryos into the micropipette and positioning embryos inside the micropipette.

B. Experiment Protocol

Mouse embryos were gathered from the Canadian Mouse Mutant Repository in the Toronto Centre for Phenogenomics. Embryos were collected 2.5 days after conception and were cultured in the KSOM medium (EMD Millipore Corporation) covered with mineral oil to prevent evaporation. After robotic vitrification, embryos were thawed and cultured to quantify the survival and development rates. All experiments followed the Kitazato vitrification protocol [15] by washing embryos in the ES solution for 10 minutes and in the VS solution for 90 seconds. After placing embryos in a different type of solution, the system immediately aspirates the solution into the micropipette to allow for sufficient diffusion of fluids inside the micropipette. After the strictly timed 90-second washing in VS, embryos must be quickly picked up from VS and deposited onto vitrification straw surfaces, and excess VS medium must be quickly aspirated away from the straw surface in order to avoid overexposure of embryos to the toxic VS solution.

III. Key Methods

A. Visual Detection of Multiple Embryos

Positions of multiple embryos are visually detected and provide visual feedback for closed-loop control [Fig. 2(b)].

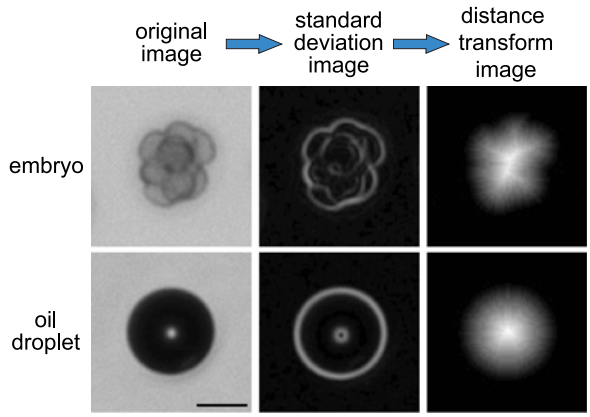

Fig. 3. Texture-based embryo detection in the x-y focal plane. Embryos reveal rough textures while the image background and oil droplets have smooth textures. Also shown are standard deviation images and distance transform images. Scale bar: 50 μm.

Visual detection includes two tasks: 2D embryo detection in culture medium where embryos all stay on culture dish bottom, and 3D embryo detection in the VS solution where embryos have different floating dynamics due to dehydration in the VS.

1) 2D detection: The culture dish is covered with mineral oil to prevent medium evaporation. Oil droplets having similar dimensions as embryos can be mistaken as embryos. Since oil droplets and embryos have different textures in images, their texture differences are used for distinguishing them. As shown in Fig. 3, the cytoplasm of cells inside an embryo shows rough textures. These rough textures are further enhanced by the pixel variance among neighboring embryonic cells, represented in standard deviation images [16]. To account for local texture, the standard deviation within a 5×5 neighborhood instead of the whole image is calculated. The 8-connected objects in the standard deviation image are marked with all holes filled. Then distance transform and binarization are applied to segment embryos according to priori knowledge of embryo size and development stages (Fig. 3). The centroid of each embryo is taken by the system as embryo position.

2) 3D detection: In the VS solution, after embryos dehydrate and shrink to their minimum volume, the toxic cryoprotectant molecules begin to diffuse into cell membrane, which can negatively affect embryo survivability. Thus, embryo processing time in the VS is much more stringent than in the ES. In order to achieve fast 3D embryo detection, the Fibonacci search algorithm [17], is applied for focus search. Focus within the region of interest of each embryo is measured by the normalized variance method because of its high accuracy and robustness to noise [18]. Position and focus data measured from multiple embryos are assigned to embryos by k-means clustering of x-y coordinates because embryos mainly float in the Z direction with little drift in the XY direction. After visual detection, the robotic system cooperatively controls the X-Y motorized stage and the micromanipulator to position the embryo at the micropipette tip for closed-loop aspiration.

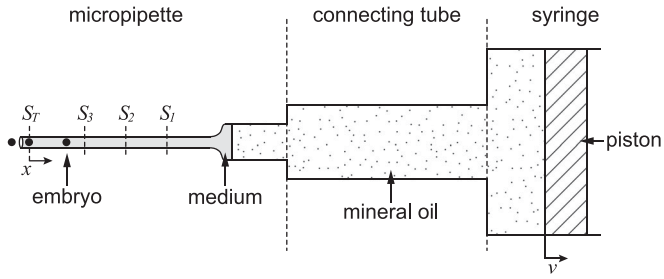

Fig. 4. Schematic diagram of controlled aspiration of multiple embryos. Each aspirated embryo is placed within 10 μm to the micropipette tip, and aspirated with a flow rate up to 16.1 nL/s. An embryo is first aspirated into the micropipette with minimum excess medium, then positioned inside the micropipette. S_T is the temporary target position for aspirating embryos into the micropipette. S_1, S_2, S_3 are preset final target position of the first, second, and third aspirated embryo, respectively.

B. Closed-Loop Aspiration

Aspiration is the process of controlling fluidic flow to position embryos into the micropipette tip [19]. The aspiration of multiple embryos is sequentially performed by repeating the control cycles of aspirating a single embryo. This sequential approach is made feasible by the fact that once an embryo enters the micropipette, its motion is confined by the micropipette wall and moves together with the medium without relative motion. However, relative motion exists outside the micropipette because of the aspiration flow. Hence, each single aspiration cycle is divided into two stages: *1)* aspirating an embryo into the micropipette, and *2)* positioning inside the micropipette the new embryo and those embryos already aspirated into the micropipette.

1) Minimum volume aspiration: Due to the relative motion between the embryo and aspirating flow, excess medium is aspirated together with the embryo. The excess medium can greatly change the position of existing embryos inside the micropipette, causing errors in position control. In order to ensure all embryos reach their final target positions, the volume of excess medium must be minimized. Therefore, the aspiration process is an optimal control problem, i.e., to aspirate the embryo to the target position S_T at micropipette tip with minimum volume of the medium aspirated.

The dynamics of embryo motion is first modelled to describe the optimal control problem. As shown later, the cost function is linear-quadratic; therefore, an LQR controller is used to solve the aspiration problem. As schematically presented in Fig. 4, velocity of the syringe piston is denoted by v. Position of the embryo is denoted by x. In the micropipette, position of an embryo is obtained from visual feedback by a motion-based tracking algorithm [20], [21]. Both the connecting tube and the syringe are filled with mineral oil, and the micropipette is filled with culture medium. According to Bernoulli's principle, motion of the piston generates a pressure P at the oil-medium interface.

$$P = \frac{1}{2}\rho v^2 + P_0 \tag{1}$$

where ρ is the density of the mineral oil, and P_0 is the atmospheric pressure. Since the culture medium segment is short,

the pressure drop between the oil-medium and the micropipette tip is negligible. The aspiration pressure at the micropipette tip equals P.

Applying Newton's law, the dynamic equation of the moving medium containing an embryo is

$$m\ddot{x} + c\dot{x} = \frac{1}{2}\rho A_p v^2 + A_p P_0 \tag{2}$$

where m is the mass of the medium at the micropipette tip containing the embryo, c is the damping of the medium, and A_p is the cross sectional area of the micropipette tip. As expressed in (2), the control input is the velocity of the piston v, and system output is the position of the embryo x. The system is first linearized to define the optimal control problem. The right-hand side of (2) is denoted as

$$u = k_p(x_d - x) + k_d(\dot{x}_d - \dot{x}) \tag{3}$$

where k_p is the proportional gain, k_d is the derivative gain, and x_d is the target embryo position. Combining (2) and (3), the control input is rewritten as

$$v = \sqrt{\frac{2}{\rho A_p}[k_p(x_d - x) + k_d(\dot{x}_d - \dot{x}) - A_p P_0]} \tag{4}$$

The state-space presentation of the system is

$$\dot{X} = AX + Bu \tag{5}$$

where

$$\dot{X} = \begin{pmatrix} x \\ \dot{x} \end{pmatrix}, A = \begin{pmatrix} 0 & 1 \\ 0 & -\dfrac{c}{m} \end{pmatrix}, B = \begin{pmatrix} 0 \\ \dfrac{1}{m} \end{pmatrix}$$

Since the aspiration position of each embryo is determined by both aspiration position error and the volume of excess medium aspirated, the aspiration problem is to find the control law of v that minimizes the cost function

$$J = x^2(t_f) + \int_{t_0}^{t_f} vA_p dt \tag{6}$$

where $x(t_f)$ is the aspiration position at terminal time t_f, t_0 is the initial time.

In (6), the integral part $\int_{t_0}^{t_f} vA_p dt$ emphasizes the total volume of excess medium aspirated, and $x^2(t_f)$ represents the error of aspiration position.

With (4) and (5), finding the minimum of (6) is equivalent to finding the minimum of the linear-quadratic function

$$J = X^T(t_f)Q_1X(t_f) + \int_{t_0}^{t_f} u^T Q_2 u dt \tag{7}$$

where Q_1, Q_2 are final state cost and control cost weight matrices, respectively.

Given that the cost function in (7) is in the linear-quadratic form and the states (i.e., embryo position x and derivative of the position $\dot{x}$) of the system are measurable, an LQR controller is applied to solve the optimal control problem. Based on the LQR theory, the control law is

$$u^* = -KX = -Q_2^{-1}B^T PX \tag{8}$$

where $K = (k_p, k_d) = Q_2^{-1}B^T P$ is the feedback parameter matrix, and the matrix P is solved from the Riccati equation

$$PA + A^T P - PBQ_2^{-1}B^T P + \dot{P} = 0 \tag{9}$$

Substituting $K = (k_p, k_d)$ into (4), the velocity of the piston v (i.e., the control input) is obtained.

2) Positioning embryos inside the micropipette: Before aspirating the next embryo, the system moves the micropipette to a region without embryos to aspirate a picoliter volume of medium to adjust the spacing between the current embryo position (S_i) and the next embryo position (S_{i+1}). According to the preset final target positions of each embryo inside the micropipette, the volume of extra medium aspirated V_{em} is calculated by $V_{em} = (S_i - S_{i+1})A_p$, where A_p is the cross sectional area of the micropipette tip. The aspiration-positioning steps are repeated until all embryos have been aspirated.

C. Placing Embryos on Vitrification Straws

After pick-and-place in the ES and the VS solutions, each processed embryo is automatically placed on an individual vitrification straw (i.e., one embryo per straw) for freezing in liquid nitrogen. The relative position between the micropipette and the vitrification straw is determined by detecting the contact between the micropipette and the vitrification straw, as we previously reported [14]. As performed in manual vitrification, the system first dispenses the embryo with VS solution on the straw, then the excess VS is removed to ensure a high cooling rate in the liquid nitrogen. When VS is aspirated back into the micropipette, friction force acts on the embryo to keep it in the original place. However, friction force varies across straws due to heterogeneity in straw surface roughness, calling for new methods to more robustly keep the embryo on the straw surface.

To more robustly keep the embryo on straw, the robotic system stretches the VS medium to a thin film on straw by moving the straw while dispensing VS medium. As schematically shown in Fig. 5(a)(b), by moving the straw, the embryo is placed away from the micropipette. A thin film is formed as the straw moves at a relatively high velocity (e.g., 400 μm/s). The embryo contacts the straw surface and friction force acts to keep the embryo in place [Fig. 5(a)(c)]. Moreover, the surface tension of the thin film also helps to keep the embryo in its original place. In contrast, when the straw is not moved or moved at a relatively low velocity (e.g., 150 μm/s), the VS medium forms a thick droplet in which the embryo floats [Fig. 5(b)(d)] and can be aspirated together with the excess VS medium back into the micropipette, causing embryo deposition to fail.

The system dynamically adjusts the straw velocity to ensure a thin film is formed. Giving a certain volume of medium $\Delta V(t)$ already dispensed on the straw at time t, film thickness h is estimated by $h = \Delta V(t)/A_f(t)$, where $A_f(t)$ is the film contour area detected in image. If h is large, the straw moves faster to stretch a thin film. Therefore, straw velocity v_s is set relative to film thickness:

$$v_s = kh = k\frac{\Delta V(t)}{A_f(t)} \tag{10}$$

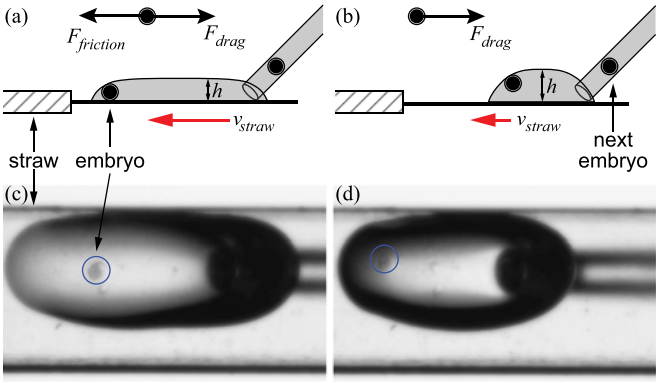

Fig. 5. (a)(b) Side view of embryo deposition on vitrification straw. (a) The straw moves to stretch the vitrification solution to a thin film, as embryo and VS medium are dispensed. The fluid drag force is balanced by the friction between the embryo and straw surface. (b) At low straw velocity, the solution forms a droplet. The embryo floats inside the droplet and friction force cannot act to keep the embryo on straw surface. (c)(d) Top view of experimental situation: liquid film on vitrification straw.

where the proportional coefficient k was experimentally determined to be 2.5 such that the straw velocity was neither too low to form a thick film in which embryos can float, nor too high to stretch the film into separate droplets. After a thin film is formed, the excess VS medium is removed and the straw with a single embryo on it is plunged into liquid nitrogen for freezing.

IV. RESULTS AND DISCUSSION

A. Visual Detection

Embryo detection success rate was quantified to evaluate the performance of visual detection. Detection was considered successful when the algorithm successfully focused on each embryo and indicated its X-Y position. Thirty visual detection experiments of 90 mouse embryos were conducted. For 2D embryo detection in culture medium, 90 out of the 90 embryos were successfully detected. Although oil droplets were present in the culture medium, none of the oil droplets was falsely detected as embryos.

For 3D detection of floating embryos in the VS solution, 86 of 90 embryos were successfully detected, yielding a success rate of 95.5%. In the four failure cases, the embryos floated close to the surface of the VS solution. At the liquid-air interface, the contrast between the embryo and background was too low for textures to be detected. Methods for increasing image contrast and predicting embryo locations based on their positions immediately before they reach the liquid-air interface are under development.

Detection speed was also measured. Due to low computational complexity, the 2D detection algorithm achieved real-time performance at 30 Hz. For 3D embryo detection, the average detection time was 3.5±0.29 seconds (mean ± standard deviation). The speed of 3D detection was limited by the motion of the focusing motor. Overall, the average detection time of 3.5 seconds is sufficient within the 90-second VS processing step,

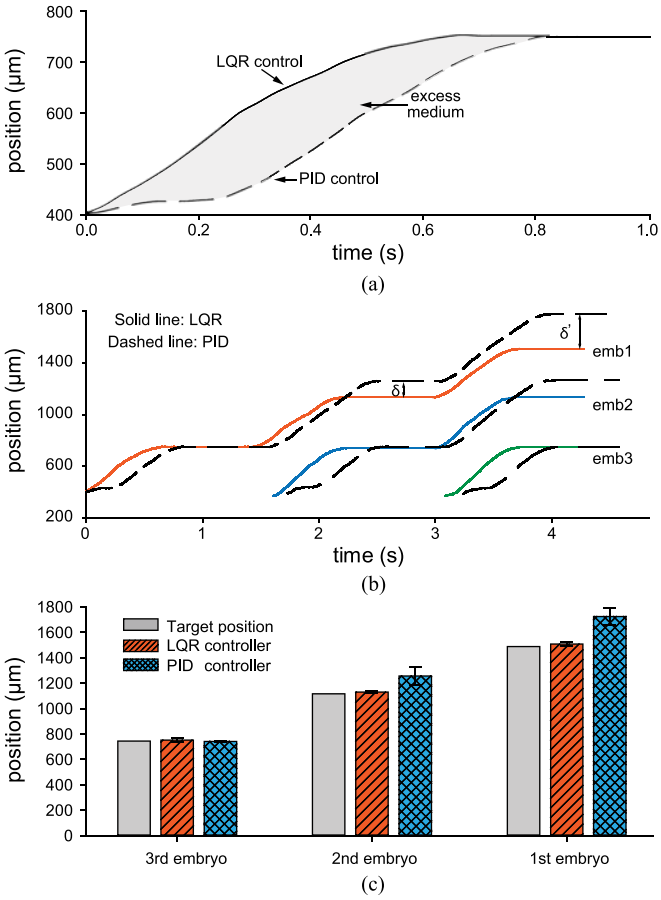

Fig. 6. (a) Experimental comparison of control response of aspirating a single embryo by LQR control and PID control. (b) Control response of aspirating three embryos. (c) Comparison of positioning errors of both controllers. Error bars are standard deviation (n=30).

for detecting the embryos and aspirating three embryos into the micropipette.

B. Closed-Loop Aspiration

Control performance of LQR control was quantitatively compared with that of PID control. For each controller, 90 embryos were aspirated in 30 experiments under the same experimental conditions. The target embryo positions inside the micropipette were set to be equally spaced. Positioning errors were monitored by measuring the spacing change. LQR controller gains were set to be $k_p = 2.54 \times 10^{-3}$ and $k_d = 1.59 \times 10^{-3}$. The PID gains were set through extensive trial and error for best experimental performance ($K_P = 9.53 \times 10^{-4}$, $K_I = 1.27 \times 10^{-4}$, and $K_D = 3.49 \times 10^{-4}$). With these gains, maximum piston velocity of 0.319 μm/s for LQR control and 0.223 μm/s for PID control was reached to achieve the desired control response.

The response of aspirating a single embryo by both controllers is shown in Fig. 6(a). LQR control had significantly shorter settling time than PID control (0.64 seconds versus 0.81 seconds). A fast control response is important for reducing the volume of VS medium. With the longer settling time of PID control, more excess medium was aspirated into the micropipette [see the gray

TABLE I
EXPERIMENTAL RESULTS OF MOUSE EMBRYO VITRIFICATION

method	success rate	survival rate	development rate
control	N/A	93.3%(14/15)	92.8%(13/14)
manual	84.2%(16/19)	75.0%(12/16)	91.7%(11/12)
robotic	95.2%(20/21)	90.0%(18/20)	88.8%(16/18)

region in Fig. 6(a)]. In contrast, LQR control was designed to minimize the excess VS medium [see (6) and (7)]. Compared with PID control, LQR control reduced the volume of excess medium by 6.23 nL, which was approximately 20 times the volume of a mouse embryo.

Excess medium aspirated using PID control caused positioning errors to the embryos that were already positioned inside the micropipette [see δ, δ' in Fig. 6(b)]. As summarized in Fig. 6(c), the average positioning error of the third embryo by PID control was as small as 4.95 μm because it was the last aspirated embryo and no more embryos or excess medium was aspirated afterwards. However, the average positioning error was 140.9 μm and 236.3 μm for the second and first embryo, respectively. With more embryos aspirated, more excess medium was also aspirated into the micropipette and positioning errors accumulated in PID control.

In contrast to the large positioning errors of PID control, LQR control achieved consistent positioning for all three embryos. Aspiration of each embryo minimized the volume of excess medium. The average positioning error for LQR control was 15.75 μm, which was less than 15% the size of embryos. Minimum volume aspiration achieved by the LQR controller enabled accurate volume control of each embryo. It also enabled the deposition of an embryo onto a vitrification straw with a minimum VS volume, thus shortening the exposure of the embryo to the toxic VS cryoprotectant for ensuring higher embryo survivability.

C. System Success Rate

An operation was considered successful when the robotic system achieved all steps of the vitrification protocol and successfully placed the processed embryos on the vitrification straws. Manual vitrification experiments were also performed by two skilled human operators. Human operators are not able to simultaneously process multiple embryos; therefore, only a single embryo was processed in the manual group.

As summarized in Table I, the robotic system achieved a significantly higher success rate than manual operation (95.2% versus 84.2%). Among the robotic vitrification of 21 embryos, 20 embryos were successfully vitrified. The only failure case in robotic operation occurred when the embryo floated in the VS and moved to the dark region of the inclined edges in the multiwell dish. For such a rare situation, the human operators also failed to locate the embryo within the given time of the protocol. Additionally, manual operation also failed when the operator lost track of the embryos floating in the VS solution and failed to aspirate the embryo. The visual detection algorithms and closed-loop aspiration control enabled the robotic system to process multiple embryos with a higher success rate than human operators.

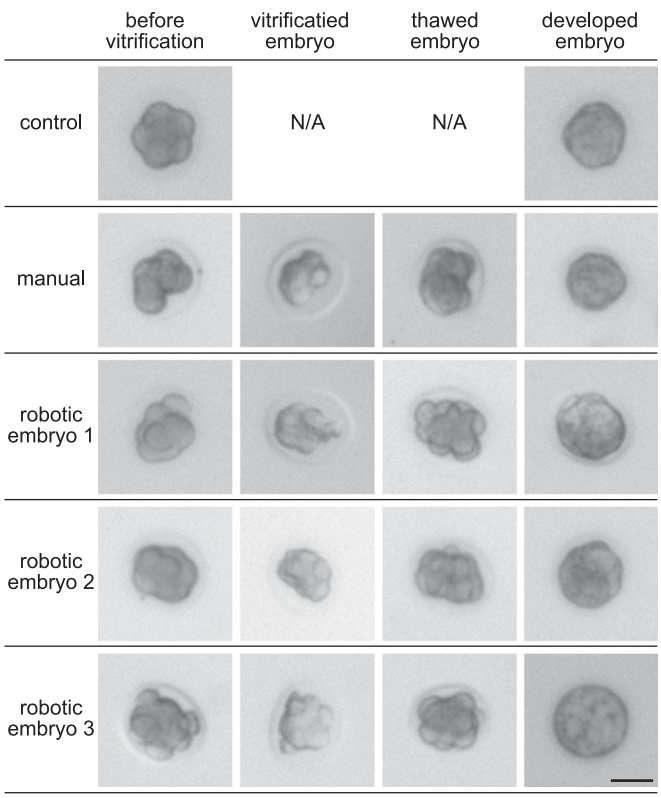

Fig. 7. Example images of fresh, vitrified, thawed, and developed embryos. Non-vitrified embryos were cultured as control group for quantifying the base development rate of the mouse embryo population. Scale bar: 50 μm.

D. Survival Rate, Development Rate, and Throughput

The post-freezing survival rate and development rate of thawed embryos were measured to further quantify the robotic system's performance. Survivability was measured by examining the morphology of embryos after thawing. According to commonly used criteria for judging embryo survivability [22], [23], an embryo was considered healthy/alive when it had no abnormal shape, membrane damage, and degeneration or fragmentation of cytoplasm. Thawed embryos were cultured for extra 24 hours for measuring their development rate. An embryo was counted as developed if it developed to the blastocyst stage [see Fig. 7]. Non-vitrified embryos were also cultured as control group for quantifying the base development rate of the mouse embryo population.

As summarized in Table I, the robotic group achieved a survival rate and a development rate close to those of the control group, indicating that the robotic vitrification process did not significantly affect embryo development potential. Embryo development potential can be affected by changes in the culture environment such as oxygen level, temperature and osmolarity. With the capability of multi-embryo processing, the robotic system shortened the time that embryos were left in the culture

medium where the culture environment can be changed by the atmosphere, thus helping maintain high embryo development potential.

The robotic group also produced a significantly higher embryo survival rate than the manual group (90.0% *versus* 75.0%). Embryo survivability was greatly affected by the overexposure to VS after the 90-second dehydration time required by the vitrification protocol. With accurate control of aspiration and deposition volume, the robotic system shortened this overexposure and achieved a higher embryo survival rate.

Simultaneously processing three embryos is faster than processing a single embryo per vitrification cycle. Following the same protocol to process 21 embryos, the single-embryo method cost approximately 315 minutes (15 minutes per embryo) while robotic operation only cost 102.9 minutes due to the capability of processing three embryos as a group. Processing more than three embryos at a time would lead to a higher system throughput; however, it would cost more time to deposit the embryos on vitrification straws and can overexpose the embryos to toxic VS solution. As a tradeoff between system throughput and embryo viability, three embryos were selected as a group in this work.

In our previous robotic vitrification system that picked and placed a single embryo at a time [14], a three times throughput compared to that of manual operation was achieved by placing several embryos at once in the ES solution for equilibration. These embryos were then washed in the VS individually and placed on vitrification straws one by one. Although the new system reported in this paper has a similar throughput as our previous system, the new system performs vitrification by strictly mimicking manual operation by clinical embryologists without letting any embryo be equilibrated longer than necessary in ES as in our previous system [14].

V. CONCLUSION

This paper presented an automated robotic vitrification system capable of pick-and-place of multiple embryos. Computer vision algorithms were developed to detect embryo positions in both 2D and 3D. An aspiration-positioning strategy was developed for controlled aspiration of multiple embryos. An LQR controller was developed to aspirate each embryo with minimum volume of excess medium. Vitrified embryos were reliably placed on the vitrification straws by taking advantage of both surface tension and friction force. These techniques enabled the robotic system to achieve a higher success rate and embryo survival rate compared to manual vitrification. The throughput of robotic multi-embryo processing is three times that of manual operation.

REFERENCES

[1] J. Liebermann, F. Nawroth, V. Isachenko, E. Isachenko, G. Rahimi, and M. J. Tucker, "Potential importance of vitrification in reproductive medicine," *Biol. Reproduction*, vol. 67, no. 6, pp. 1671–1680, 2002.

[2] A. Dhali, V. M. Anchamparuthy, S. P. Butler, R. E. Pearson, I. K. Mullarky, and F. C. Gwazdauskas, "Effect of droplet vitrification on development competence, actin cytoskeletal integrity and gene expression in in vitro cultured mouse embryos," *Theriogenology*, vol. 71, no. 9, pp. 1408–1416, 2009.

[3] H. Selman, A. Angelini, N. Barnocchi, G. F. Brusco, A. Pacchiarotti, and C. Aragona, "Ongoing pregnancies after vitrification of human oocytes using a combined solution of ethylene glycol and dimethyl sulfoxide," *Fertility Sterility*, vol. 86, no. 4, pp. 997–1000, 2006.

[4] S. F. Mullen, M. Li, Y. Li, Z. J. Chen, and J. K. Critser, "Human oocyte vitrification: the permeability of metaphase II oocytes to water and ethylene glycol and the appliance toward vitrification," *Fertility Sterility*, vol. 89, no. 6, pp. 1812–1825, 2008.

[5] S. F. Mullen, M. Rosenbaum, and J. K. Critser, "The effect of osmotic stress on the cell volume, metaphase II spindle and developmental potential of in vitro matured porcine oocytes," *Cryobiology*, vol. 54, no. 3, pp. 281–289, 2007.

[6] T. Fujita, H. Umeki, H. Shimura, K. Kugumiya, and K. Shiga, "Effect of group culture and embryo-culture conditioned medium on development of bovine embryos," *J. Reproduction Develop.*, vol. 52, no. 1, pp. 137–142, 2006.

[7] J. Melin, A. Lee, K. Foygel, D. E. Leong, S. R. Quake, and M. W. M. Yao, "In vitro embryo culture in defined, sub-microliter volumes," *Developmental Dyn.*, vol. 238, no. 4, pp. 950–955, 2009.

[8] U. Waldenström, A.-B. Engström, D. Hellberg, and S. Nilsson, "Low-oxygen compared with high-oxygen atmosphere in blastocyst culture, a prospective randomized study," *Fertility Sterility*, vol. 91, no. 6, pp. 2461–2465, 2009.

[9] A. Lourens, H. van den Brand, R. Meijerhof, and B. Kemp, "Effect of eggshell temperature during incubation on embryo development, hatchability, and posthatch development," *Poultry Sci.*, vol. 84, no. 6, pp. 914–920, 2005.

[10] E. Popova, M. Bader, and A. Krivokharchenko, "Effect of culture conditions on viability of mouse and rat embryos developed in vitro," *Genes*, vol. 2, no. 2, pp. 332–344, 2011.

[11] G. Vajta, "Vitrification in human and domestic animal embryology: Work in progress," *Reproduction, Fertility Develop.*, vol. 25, no. 5, pp. 719–727, 2013.

[12] D. G. Pyne, J. Liu, M. Abdelgawad, and Y. Sun, "Digital microfluidic processing of mammalian embryos for vitrification," *PLoS ONE*, vol. 9, no. 9, pp. 1–7, 2014.

[13] Y. S. Heo *et al.*, "Controlled loading of cryoprotectants (CPAs) to oocyte with linear and complex CPA profiles on a microfluidic platform," *Lab Chip*, vol. 11, no. 20, pp. 3530–3537, 2011.

[14] J. Liu *et al.*, "Automated vitrification of embryos: A robotics approach," *IEEE Robot. Autom. Mag.*, vol. 22, no. 2, pp. 33–40, Jun. 2015.

[15] M. Kuwayama, "Highly efficient vitrification for cryopreservation of human oocytes and embryos: The Cryotop method," *Theriogenology*, vol. 67, no. 1, pp. 73–80, 2007.

[16] C. Y. Wong and J. K. Mills, "Automation and optimization of multi-pulse laser zona drilling of mouse embryos during embryo biopsy," *IEEE Trans. Biomed. Eng.*, vol. PP, no. 99, pp. 1–1, 2016, DOI: 10.1109/TBME.2016.2571060.

[17] X. Y. Liu, W. H. Wang, and Y. Sun, "Dynamic evaluation of autofocusing for automated microscopic analysis of blood smear and pap smear," *J. Microsc.*, vol. 227, no. 1, pp. 15–23, 2007.

[18] Y. Sun, S. Duthaler, and B. J. Nelson, "Autofocusing in computer microscopy: Selecting the optimal focus algorithm," *Microsc. Res. Techn.*, vol. 65, no. 3, pp. 139–149, 2004.

[19] X. P. Zhang, C. Leung, Z. Lu, N. Esfandiari, R. F. Casper, and Y. Sun, "Controlled aspiration and positioning of biological cells in a micropipette," *IEEE Trans. Biomed. Eng.*, vol. 59, no. 4, pp. 1032–1040, Apr. 2012.

[20] Z. Zhang *et al.*, "Human sperm rheotaxis: a passive physical process," *Sci. Rep.*, vol. 6, 2016, Art. no. 23553.

[21] Z. Lu, X. Zhang, C. Leung, N. Esfandiari, R. F. Casper, and Y. Sun, "Robotic ICSI (intracytoplasmic sperm injection)," *IEEE Trans. Biomed. Eng.*, vol. 58, no. 7, pp. 2102–2108, Jul. 2011.

[22] J. Zhang *et al.*, "Vitrification of mouse embryos at 2-cell, 4-cell and 8-cell stages by cryotop method," *J. Assisted Reproduction Genetics*, vol. 26, no. 11-12, pp. 621–628, 2009.

[23] M. Kuwayama, "Highly efficient vitrification for cryopreservation of human oocytes and embryos: The Cryotop method," *Theriogenology*, vol. 67, no. 1, pp. 73–80, 2007.